Letter

Intermediate-scale theory for electrons coupled to frustrated local moments

Adam J. McRoberts,[1,*] J. F. Mendez-Valderrama,[2,*] Roderich Moessner,[1] and Debanjan Chowdhury[2]
[1]*Max-Planck-Institut für Physik komplexer Systeme, Nöthnitzer Straße 38, 01187 Dresden, Germany*
[2]*Department of Physics, Cornell University, Ithaca, New York 14853, USA*

(Received 31 August 2022; accepted 19 December 2022; published 6 January 2023)

A classic route for destroying long-lived electronic quasiparticles in a weakly interacting Fermi liquid is to couple them to other low-energy degrees of freedom that effectively act as a bath. We consider here the problem of electrons scattering off the spin fluctuations of a geometrically frustrated antiferromagnet, whose nonlinear Landau-Lifshitz dynamics, which remains nontrivial at all temperatures, we model in detail. At intermediate temperatures and in the absence of any magnetic ordering, the fluctuating local moments lead to a nontrivial angular anisotropy of the scattering rate along the Fermi surface, which disappears with increasing temperature, elucidating the role of "hot spots." Over a remarkably broad window of intermediate and high temperatures, the electronic properties can be described by employing a *local* approximation for the dynamical spin response. This we contrast with the more familiar setup of electrons scattering off classical phonons, whose high-temperature limit differs fundamentally on account of their unbounded Hilbert space. We place our results in the context of layered magnetic delafossite compounds.

DOI: 10.1103/PhysRevB.107.L020402

Introduction. Electronic solids provide a fascinating experimental platform for studying the properties of an electronic fluid coupled to a "bath." A paradigmatic example is the coupled electron-phonon problem, where the phonons effectively act as a bath with which the electrons exchange energy and momentum [1]. The transport and single-particle properties for numerous metals at intermediate temperatures can be understood in terms of this "semiquantum" system over $\omega_D \lesssim T \ll \varepsilon_F$, where ε_F is the electronic Fermi energy and ω_D is a characteristic Debye frequency. A number of recent developments in moiré materials [2–7] and magnetic delafossites [8–18] inspire us to examine the following question: What is the nature of a weakly correlated electronic fluid coupled to interacting local moments for $J \lesssim T \ll \varepsilon_F$, where J is a characteristic antiferromagnetic exchange energy scale? While this system exhibits a familiar resemblance to the electron-phonon problem, there are a number of important conceptual differences.

First and foremost, spins have a bounded Hilbert space. While phonon modes tend to obey classical equipartition at high $T \gtrsim \omega_D$, spin excitations at $T \gtrsim J$ do not. Second, the dynamical correlations in an interacting ("cooperative") paramagnet at $T \gtrsim J$ are *a priori* nontrivial, arising from a nonlinear dynamics, even though the static correlations vanish asymptotically at high temperatures. Finally, residual short-range order, reflecting any magnetic order at $T < T_N$ ($\lesssim J$), can leave an imprint on the electronic properties even once the order melts at $T \gtrsim J$.

In this Letter, we focus specifically on the case of local moments with geometrically frustrated interactions on the triangular lattice [19]. A frustrated magnet is a useful starting point as a bath, since the tendency towards any long-range magnetic ordering is naturally suppressed, providing a broad paramagnetic regime, which always has a nontrivial (nonlinear) dynamics, with a momentum dependence reflecting, e.g., spin diffusion. Even at the highest temperatures, the question naturally arises whether this can impart non- (or marginal-) Fermi-liquid-like electronic correlations [20,21]. Notably, by carrying out a detailed analysis of the nonlinear spin dynamics and its effect on the electronic properties, the numerically evaluated electron self-energy can be captured quantitatively over a broad energy window $J \lesssim T \leqslant \infty$ by employing a local approximation for the spins.

Model. We consider a simple two-dimensional model of itinerant spinful electrons $c_{k\sigma}$ interacting with spin-$\frac{1}{2}$ local moments $\mathbf{S}_i$ on the sites of a triangular lattice,

$$H = H_c + H_S + H_K, \tag{1a}$$

$$H_c = \sum_{\boldsymbol{k},\sigma} (\varepsilon_{\boldsymbol{k}} - \mu) c^\dagger_{\boldsymbol{k}\sigma} c_{\boldsymbol{k}\sigma}, \quad H_S = J \sum_{\langle i,j \rangle} \mathbf{S}_i \cdot \mathbf{S}_j, \tag{1b}$$

$$H_K = g \sum_{i,\alpha,\beta} c^\dagger_{i\alpha} (\mathbf{S}_i \cdot \boldsymbol{\sigma}_{\alpha\beta}) c_{i\beta}, \tag{1c}$$

where $\varepsilon_{\boldsymbol{k}}, \mu$ represent the dispersion and chemical potential associated with the c electrons, $J(>0)$ denotes the antiferromagnetic exchange interaction between local moments, and $g(>0)$ is the Kondo coupling between the local moment and electron spin density, respectively. For the electronic dispersion, we include first (t) and second (t') neighbor hoppings on the triangular lattice. We note at the outset that in the temperature window of interest and for a "weak" Kondo coupling, the intrinsic quantum mechanical Kondo physics associated with the quenching of the local moment will be irrelevant.

[*]These authors contributed equally to this work.

The dynamics of frustrated magnets in their cooperative paramagnetic phase tends to be well described by the classical Landau-Lifshitz equations of motion governed by H_S, even for small spin lengths S far from the classical limit $S \to \infty$ [22–29]:

$$\dot{\mathbf{S}}_i = \frac{\partial H_S}{\partial \mathbf{S}_i} \times \mathbf{S}_i. \tag{2}$$

We hence approximate the spins as $O(3)$ vectors precessing around their local exchange fields, which we analyze by performing molecular dynamics (MD) simulations. We average over initial configurations obtained from classical Monte Carlo (MC) simulations of H_S and numerically integrate the equations of motion [30].

In this Letter, we analyze the extent to which the dynamical correlations associated with the fluctuating local moments leave an imprint on the electronic liquid at intermediate-energy scales. Specifically, we calculate the $O(g^2)$ perturbative correction to the electron self-energy, which is controlled by the two-point correlator of the spins. Since the primary goal is to understand the electronic properties, we ignore the electron backaction on the local moments, which affects the electronic properties at higher order in g. Previous work [31] has analyzed this problem in a different regime, focusing on the elastic transport lifetimes.

Spin dynamics. In momentum space, the two-point correlator of interest is the dynamical structure factor,

$$\mathcal{S}(\boldsymbol{q}, \omega) = \int_{-\infty}^{\infty} dt e^{i\omega t} \langle \mathbf{S}(\boldsymbol{q}, t) \cdot \mathbf{S}(-\boldsymbol{q}, 0) \rangle. \tag{3}$$

We use heat bath Monte Carlo [32] to draw an ensemble of 1000 independent initial states $\mathbf{S}_i(0)$ from the canonical ensemble of H_S at a given temperature T; from here on we measure T in units of J. The time evolution of each state is obtained by numerical integration of Eq. (2), using the standard fourth-order Runge-Kutta procedure, to a final time of $t_f = 4096 J^{-1}$. We construct each Fourier transformed state $\mathbf{S}(\boldsymbol{q}, \omega)$, whose ensemble average yields the dynamical structure factor. The numerically evaluated static structure factor, $\mathcal{S}(\boldsymbol{q}) = \int d\omega \, \mathcal{S}(\boldsymbol{q}, \omega)$, is shown for $T = J$ and $T = 10J$ in Figs. 1(a) and 1(b), respectively. The broadened "Bragg-like" peaks at $T = J$ near the high-symmetry points represent a remnant of the thermally disordered 120° antiferromagnetic state on the triangular lattice.

We are interested in the regime where the spin bandwidth—the range of frequencies over which $\mathcal{S}(\boldsymbol{q}, \omega)$ has support—is much smaller than the electronic bandwidth and Fermi energy. As we discuss later, the energy scales that are relevant for electrons with momentum $\boldsymbol{k}$ and frequency ω scattering off the spins enter the structure factor as $\mathcal{S}(\boldsymbol{q}, \omega - \varepsilon_{\boldsymbol{k}+\boldsymbol{q}})$; the latter has support only over a very narrow (and $\boldsymbol{k}$-dependent) region of momentum $\boldsymbol{q}$. Even for relatively large system sizes ($N = L^2$, $L = 120$), the momentum resolution available from the numerical simulations directly is insufficient to determine the electronic lifetime. We therefore construct an analytical fit to $\mathcal{S}(\boldsymbol{q}, \omega)$ from our numerics.

We obtain the static (equal-time) structure factor from a "soft spin" approximation [30]. We can then describe the numerically computed dynamical structure factor, for $T \gtrsim J$,

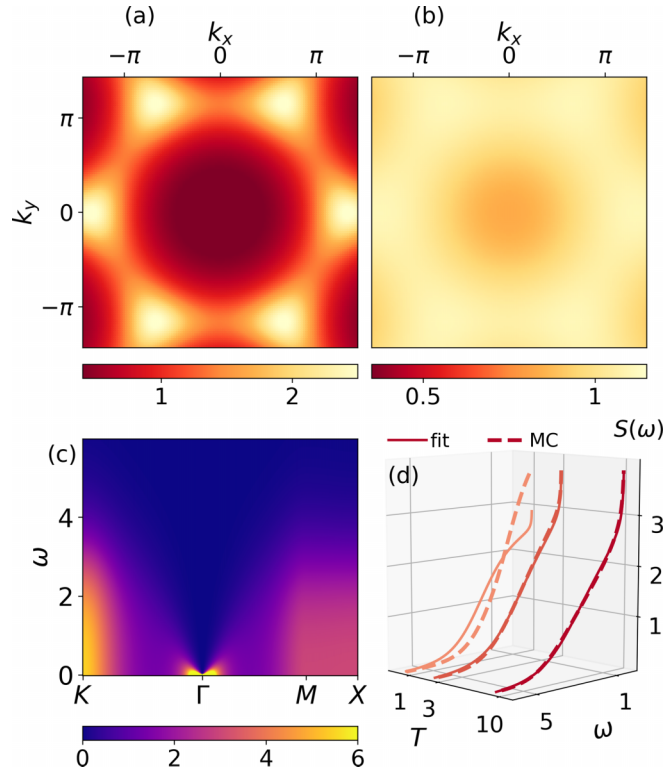

FIG. 1. The static structure factor $\mathcal{S}(\boldsymbol{q})$ over the Brillouin zone for (a) $T = J$, and (b) $T = 10J$, respectively. (c) $\mathcal{S}(\boldsymbol{q}, \omega)$ over a momentum cut $K \to \Gamma \to M \to X$, at $T = 3J$. (d) The momentum-integrated structure factor for selected temperatures, together with the fit in Eq. (4).

using the following phenomenological ansatz,

$$\mathcal{S}(\boldsymbol{q}, \omega) = \frac{\mathcal{S}(\boldsymbol{q}) \mathcal{N}(\alpha_{\boldsymbol{q}}, \eta_{\boldsymbol{q}})}{\sinh^2(\alpha_{\boldsymbol{q}} \omega) + \eta_{\boldsymbol{q}}}, \tag{4}$$

where $\alpha_{\boldsymbol{q}}$ and $\eta_{\boldsymbol{q}}$ are momentum-dependent fitting parameters, and $\mathcal{N}$ is a normalization factor enforcing $\mathcal{S}(\boldsymbol{q}) = \int d\omega \, \mathcal{S}(\boldsymbol{q}, \omega)$. As both $\alpha_{\boldsymbol{q}}$, $\eta_{\boldsymbol{q}}$ respect the space group symmetries of the triangular lattice, they can be expressed in terms of the following objects,

$$\gamma_n(\boldsymbol{q}) = \frac{1}{|E_n|} \sum_{\boldsymbol{\delta} \in E_n} e^{i\boldsymbol{q} \cdot \boldsymbol{\delta}}, \tag{5}$$

where E_n is the set of nth nearest-neighbor vectors, and $|E_n|$ its cardinality. At high temperature, with a short correlation length, typically the first few γ_n are sufficient to describe these fit functions. We show $\mathcal{S}(\boldsymbol{q}, \omega)$ along a certain high-symmetry cut in the Brillouin zone at $T = 3J$ in Fig. 1(c). In Fig. 1(d) we compare our analytical fit functions to the momentum-integrated structure factors for three different temperatures. As expected, the quality of our fits improves with increasing temperature; the largest disagreement can be seen at $T = J$.

Electron self-energy. The imaginary part of the electron self-energy at real frequencies is given by

$$\Sigma''(\boldsymbol{k}, \omega) = \frac{g^2}{N} \sum_{\boldsymbol{q}} \int \frac{d\Omega}{\pi} \chi''_{\text{spin}}(\boldsymbol{q}, \omega - \varepsilon_{\boldsymbol{k}+\boldsymbol{q}}) A_c \times (\boldsymbol{k} + \boldsymbol{q}, \Omega) f(\omega, \Omega), \tag{6a}$$

$$f(\omega, \Omega) = [n_b(\omega - \Omega) + n_f(-\Omega)], \tag{6b}$$

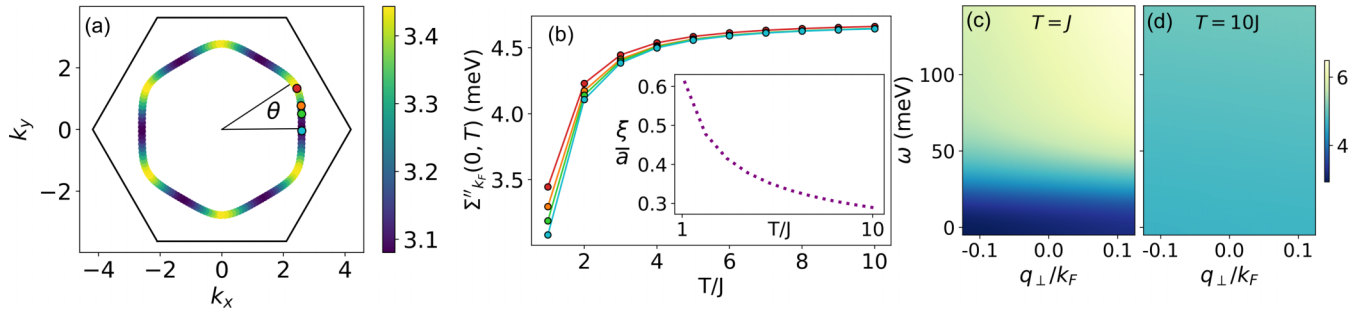

FIG. 2. The numerically evaluated electron self-energy $\Sigma''_{k_F}(0,T)$ (a) along the Fermi surface at $T=J$, and (b) for different θ along the Fermi surface as a function of temperature. Inset: The spin correlation length $\xi(T)$ extracted from $\mathcal{S}(\boldsymbol{q})$. (c), (d) With increasing temperature, $\Sigma''_{k_F}(q_\perp,\omega)$ becomes featureless as a function of both ω and $q_\perp$.

where $A_c(\boldsymbol{k},\omega)$ is the electron spectral function, $\chi''_{\rm spin}(\boldsymbol{k},\omega)$ denotes the imaginary part of the spin susceptibility, and $n_b(\dots), n_f(\dots)$ denote the Bose-Einstein and Fermi-Dirac distributions at temperature $T=\beta^{-1}$, respectively. In the temperature window of interest, the susceptibility is related to the structure factor discussed earlier,

$$\chi''_{\rm spin}(\boldsymbol{q},\omega)=\beta\omega\mathcal{S}(\boldsymbol{q},\omega), \tag{7}$$

where we have used the high-temperature ("classical") version of the fluctuation-dissipation theorem for the sake of internal consistency [30]. In what follows, a key new ingredient in our computation is associated with a detailed microscopic modeling of the intermediate-scale nonlinear dynamics of the spin system, which can modify the electron self-energy in interesting ways.

We begin by noting that, despite the small spin bandwidth, high-energy electrons ($\omega\gg J$) can scatter off the spins as long as $|\omega-\varepsilon_{\boldsymbol{k}}|\lesssim J$. We first evaluate the self-energy numerically [30]. In what follows, we fix $t=568$ meV, $t'=-108$ meV, $J=10.34$ meV, $g=2.5$ meV, and $\mu=247.5$ meV. These values are partly inspired by the magnetic delafossite $PdCrO_2$ [17], which consists of alternately stacked layers of triangular lattice antiferromagnetic Mott insulators and weakly correlated metals near half filling. The electronic transport properties in this compound are clearly affected by the presence of thermally fluctuating local moments [33], which necessitates a theoretical investigation of the single-particle lifetime in this unusual regime.

Numerical results. The results for $\Sigma''_{k_F}(\omega=0,T)$ around the Fermi surface with $|\boldsymbol{k}|=k_F$ for a number of angles θ and over a range of finite temperatures is shown in Figs. 2(a) and 2(b). There are six bright spots at $T\gtrsim J$, that we associate with hot regions arising from scattering off short-ranged magnetic fluctuations with a finite correlation length $\xi(T)$, peaked near the $\boldsymbol{K},\boldsymbol{K}'$ points in the Brillouin zone (BZ). These regions comprise 12 "hot spots" identified by the condition $\varepsilon(\boldsymbol{k}\pm\boldsymbol{K})=\varepsilon(\boldsymbol{k})$ (similarly for $\boldsymbol{K}'$), that become thermally smeared into the six spots [30].

The behavior is reminiscent of fluctuation effects involving electrons scattering off short-ranged density-wave fluctuations in the context of a Peierls transition in one dimension [34]. Furthermore, the angular variation of the evaluated self-energy is closely tied to the filling, and the magnitude of the $2k_F$ vector relative to the ordering wave vectors [30]. With increasing temperature, the angular anisotropy near the hot spots disappears as the correlation length decreases. Ultimately, with increasing T, and in contrast to electrons scattering off high-temperature phonons, there appears a uniform temperature-independent saturation value for the self-energy along the Fermi surface associated with the asymptotic limit $J\ll T(\ll\varepsilon_F)$; see Fig. 2(b). However, this saturation sets in gently, with $\Sigma''_{k_F}(\omega=0,T)$ varying only within ≈20% of its saturation value between $T=J$ and $T=10J$. We extract the spin correlation length $\xi(T)$ from the real space static structure factor as a function of increasing temperature, and find that it is already smaller than the lattice spacing at $T=J$.

Next, we evaluate the frequency and (transverse) momentum dependence of the self-energy, $\Sigma''_{k_F}(q_\perp,\omega,T)$, away from the Fermi surface. In Figs. 2(c) and 2(d), we show a color map for the self-energy for a fixed θ at two different temperatures; the scales are chosen such that ω is comparable to $v_F q_\perp$. At $T\sim J$, the self-energy exhibits a weak $q_\perp$ dependence; the interesting feature is tied to the ω dependence for the full range of $q_\perp$ considered in Fig. 2(c). At a fixed $q_\perp$, $\Sigma''_{k_F}(\omega)\sim\omega^2$ at low frequencies, and crosses over into a distinct regime with weak ω dependence for $\omega\gtrsim 2J$. With increasing temperature [Fig. 2(d)], the self-energy becomes largely momentum independent, signaling a predominantly "local" character of the spin-fluctuation spectrum. In such a regime, the self-energy displays a nearly featureless behavior as a function of ω, $q_\perp$, that varies weakly with temperature. The electronic properties for $3J\lesssim T\ll\varepsilon_F$ can be captured by the high-temperature and local limit of $\chi''_{\rm spin}$, as we discuss below.

In Fig. 3(a), we analyze the ω and T dependence of Σ''_{k_F} for a range of θ along the Fermi surface. At low T, there is a crossover from a ω^2 to a weak ω dependence at larger ω; the dispersive structure disappears with increasing T. Despite the angular anisotropy in $\Sigma''_{k_F}(\omega=0,T)$ for small T, the relative renormalization of the self-energy as a function of ω is largely insensitive to θ at a given T. We have also observed that even for finite $q_\perp$, the ω,T dependencies are broadly similar to the $q_\perp=0$ results. In spite of the complex structure of the dynamical spin response (Fig. 2), we will be able to capture most of the *quantitative* features of the electron self-energy starting from a high-temperature analytical perspective.

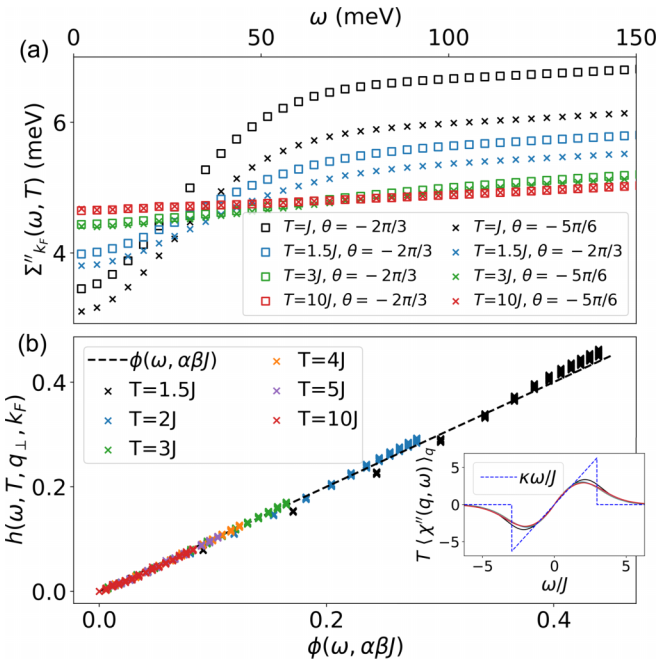

FIG. 3. (a) Frequency dependence of the self-energy at different angles along the Fermi surface with increasing temperature. (b) The function $h(\dots)$ constructed out of the electron self-energy [Eq. (10)] exhibits a scaling collapse on a universal momentum-independent curve $\phi(\omega, \alpha\beta J)$ over a wide range of T, angle around the Fermi surface, and $q_\perp$.

Analytical approach for electron self-energy. Recall that, in the Lehmann representation,

$$\chi''_{\rm spin}(\boldsymbol{q},\omega) = \pi(e^{\beta\omega}-1)\frac{1}{Z}\sum_{n,m,\alpha} e^{-\beta E_m}\left|\langle n|S^\alpha_{\boldsymbol{q}}|m\rangle\right|^2 \times\delta(\omega+E_n-E_m), \tag{8}$$

where the $\{n, E_n\}$ label the many-body eigenstates and eigenenergies, respectively, and Z is the partition function. The spin operators $S^\alpha_{\boldsymbol{q}}$ denote the α component with momentum $\boldsymbol{q}$. Remarkably, we have observed that the numerical computation of the electron self-energy based on the full $\mathcal{S}(\boldsymbol{q},\omega)$ agrees almost perfectly with a completely "local" approximation for the susceptibility (to be made precise below). Specifically, this implies that the frequency and angular dependence along the Fermi surface of the electron self-energy is controlled by the nearly momentum-independent, nondiffusive piece of the structure factor [30]. We can quantitatively account for this behavior at $T \gtrsim J$ based on a simple (but controlled) "local" approximation for $\chi''_{\rm spin}$, which is reminiscent of a dynamical mean-field theory-type approximation [35]. Instead of ignoring the $\boldsymbol{q}$ dependence of the matrix elements in Eq. (8) altogether, we replace it by a momentum average that leads to an overall constant prefactor κ, with $\chi''_{\rm spin} \approx \kappa\beta\omega/J$. This is also consistent with our direct computations of $\chi''_{\rm spin}$ extracted from $\mathcal{S}(\boldsymbol{q},\omega)$ at small ω [Fig. 3(b) inset]. We emphasize that there is a crossover out of the $\chi''_{\rm spin} \sim \omega$ regime and the response vanishes smoothly beyond a scale set by the spin bandwidth, which for tractability we replace with a sharp cutoff at $|\omega| = \alpha\pi J$ [30]. We use the above approximate form to simplify the local electron self-energy as

$$\Sigma''_{\rm loc}(\omega, T) \approx \int d\varepsilon\, \nu(\varepsilon)\chi''_{\rm spin}(\omega-\varepsilon)f(\omega,\varepsilon), \tag{9}$$

where $\nu(\varepsilon)$ is the electronic density of states and $f(\omega,\varepsilon)$ is as defined in Eq. (6a). We use the simplified form of $\chi''_{\rm spin}$ introduced above.

To better characterize the ω dependence of the numerically evaluated self-energy with increasing temperature, accounting for the intrinsic variations associated with $\Sigma''_{k_F}(0, T)$, we consider the function

$$h(\omega, T, q_\perp, k_F) = \frac{\Sigma''_{k_F}(q_\perp,\omega,T)}{\Sigma''_{k_F}(q_\perp,0,T)} - 1, \tag{10}$$

which trivially satisfies $h(\omega = 0, T, q_\perp, k_F) = 0$. We have evaluated $h(\omega, T, q_\perp, k_F)$ for a range of temperatures, $1.5J \leqslant T \leqslant 10J$, for six different $\theta \in [0, \pi/6]$ along the Fermi surface, and for the same range of $q_\perp$ as in Figs. 2(c) and 2(d). Remarkably, we find that these curves all collapse on to a universal function, $\phi(\omega, \alpha\beta J)$ [dashed line in Fig. 3(b)], that is computed using the local form of the spin susceptibility in Eq. (9). The explicit analytical form for $\phi(\omega, \alpha\beta J)$ appears in the Supplemental Material [30]. Note that the only free parameter here is α, which fixes the spin bandwidth, and can reproduce the curves for all $T \gtrsim J$ and a wide range of ω; αJ also sets the scale at which $\Sigma''_{\rm loc}(\omega)$ crosses over from a low-frequency ω^2 behavior to the asymptotic high-frequency regime. Moreover, when $\beta\omega \to 0$ and $\beta\alpha J \ll 1$, the coefficient of this low-frequency regime scales as $\Sigma''_{\rm loc}(\omega) \sim \beta^4\omega^2$ (with additional dimensionful prefactors) [30]. We note that the dashed line in Fig. 3(b) captures the full β dependence and various crossovers out of the asymptotic high-temperature regime.

It has not escaped our attention that at large frequencies, there is a weak ω-linear dependence of $\Sigma''_{k_F}(\omega) \sim \Sigma''_{\rm loc}(\omega)$, whose slope is independent of temperature. For the specific electronic dispersion on the triangular lattice near half filling that is used to evaluate the self-energy, we are near a van Hove singularity. The origin of this frequency dependence can be traced back to the electronic density of states $\nu(\omega)$, which is not independent of ω [30].

Contrast with electron-phonon scattering. It is useful to contrast the results obtained here for electrons scattering off a frustrated paramagnet with the more conventional example of electron-phonon scattering at $\omega_{\rm D} < T \ll \varepsilon_{\rm F}$. As a function of frequency, the two problems are similar, with $\omega_{\rm D}$ playing a role analogous to the spin bandwidth. However, due to the unbounded phonon Hilbert space and an associated temperature-independent phonon spectral function, we note that, at low frequencies, $\Sigma''_{\rm loc}(\omega)/\Sigma''_{\text{el-ph}}(\omega) \sim \beta$ [30]. Similarly, as is already clear from our considerations thus far, in the high-T limit and for $\omega = 0$ we also find $\Sigma''_{\rm loc}(T)/\Sigma''_{\text{el-ph}}(T) \sim \beta$. This is consistent with the classical result, whereby electrons scattering off high-temperature phonons leads to a scattering cross section that depends linearly on temperature. On the other hand, the additional suppression of the spin spectral function ($\sim\beta$) exactly cancels out this temperature dependence.

Outlook. We have presented a quantitative theory for the electron self-energy for $J \lesssim T \leqslant \infty$ in a Fermi liquid when Kondo coupled to a frustrated Heisenberg spin system obeying semiclassical Landau-Lifshitz dynamics. The resulting electron self-energy leads to a conundrum for the in-plane electrical transport in $PdCrO_2$, which displays a broad regime of an excess T-linear resistivity for $T \gtrsim J$, when compared against the isostructural but nonmagnetic compound $PdCoO_2$ [33]. The distinction to $PdCoO_2$ would seem to rule out a purely electron-phonon scenario, as well as a scenario involving electrons scattering off spin waves [36]. Our present analysis disfavors an analogous electron–local-moment scenario. Identifying the origin of this phenomenon remains a worthwhile challenge.

Acknowledgments. We thank E. Berg, A. Mackenzie, and V. Sunko for discussions. J.F.M.V. and D.C. are supported by faculty startup funds at Cornell University. D.C. acknowledges the hospitality of the Max-Planck Institute for the Physics of Complex Systems during the final stages of this work. This work was in part supported by the Deutsche Forschungsgemeinschaft under Grant No. SFB 1143 (project-id 247310070) and the cluster of excellence ct.qmat (EXC 2147, project-id 390858490).

[1] J. M. Ziman, *Electrons and Phonons: The Theory of Transport Phenomena in Solids* (Oxford University Press, Oxford, UK, 1960).

[2] D. M. Kennes, M. Claassen, L. Xian, A. Georges, A. J. Millis, J. Hone, C. R. Dean, D. N. Basov, A. N. Pasupathy, and A. Rubio, Moiré heterostructures as a condensed-matter quantum simulator, Nat. Phys. **17**, 155 (2021).

[3] K. F. Mak and J. Shan, Semiconductor moiré materials, Nat. Nanotechnol. **17**, 686 (2022).

[4] T. Li, S. Jiang, L. Li, Y. Zhang, K. Kang, J. Zhu, K. Watanabe, T. Taniguchi, D. Chowdhury, L. Fu, J. Shan, and K. F. Mak, Continuous Mott transition in semiconductor moiré superlattices, Nature (London) **597**, 350 (2021).

[5] A. Ghiotto, E.-M. Shih, G. S. S. G. Pereira, D. A. Rhodes, B. Kim, J. Zang, A. J. Millis, K. Watanabe, T. Taniguchi, J. C. Hone, L. Wang, C. R. Dean, and A. N. Pasupathy, Quantum criticality in twisted transition metal dichalcogenides, Nature (London) **597**, 345 (2021).

[6] A. Kumar, N. Chao Hu, A. H. MacDonald, and A. C. Potter, Gate-tunable heavy fermion quantum criticality in a moiré Kondo lattice, Phys. Rev. B **106**, L041116 (2022).

[7] A. Dalal and J. Ruhman, Orbitally selective Mott phase in electron-doped twisted transition metal-dichalcogenides: A possible realization of the Kondo lattice model, Phys. Rev. Res. **3**, 043173 (2021).

[8] A. P. Mackenzie, The properties of ultrapure delafossite metals, Rep. Prog. Phys. **80**, 032501 (2017).

[9] H. Takatsu, S. Yonezawa, C. Michioka, K. Yoshimura, and Y. Maeno, Anisotropy in the magnetization and resistivity of the metallic triangular-lattice magnet $PdCrO_2$, J. Phys.: Conf. Ser. **200**, 012198 (2010).

[10] K. P. Ong and D. J. Singh, Three-dimensional magnetism and coupling to the conduction electrons in $PdCrO_2$, Phys. Rev. B **85**, 134403 (2012).

[11] A. Glamazda, W.-J. Lee, S.-H. Do, K.-Y. Choi, P. Lemmens, J. van Tol, J. Jeong, and H.-J. Noh, Collective excitations in the metallic triangular antiferromagnet $PdCrO_2$, Phys. Rev. B **90**, 045122 (2014).

[12] H. Takatsu, G. Nénert, H. Kadowaki, H. Yoshizawa, M. Enderle, S. Yonezawa, Y. Maeno, J. Kim, N. Tsuji, M. Takata *et al.*, Magnetic structure of the conductive triangular-lattice antiferromagnet $PdCrO_2$, Phys. Rev. B **89**, 104408 (2014).

[13] H.-J. Noh, J. Jeong, B. Chang, D. Jeong, H. S. Moon, E.-J. Cho, J. M. Ok, J. S. Kim, K. Kim, B. Min *et al.*, Direct observation of localized spin antiferromagnetic transition in $PdCrO_2$ by angle-resolved photoemission spectroscopy, Sci. Rep. **4**, 3680 (2014).

[14] R. Daou, R. Frésard, V. Eyert, S. Hébert, and A. Maignan, Unconventional aspects of electronic transport in delafossite oxides, Sci. Technol. Adv. Mater. **18**, 919 (2017).

[15] D. Sun, D. A. Sokolov, J. M. Bartlett, J. Sannigrahi, S. Khim, P. Kushwaha, D. D. Khalyavin, P. Manuel, A. S. Gibbs, H. Takagi *et al.*, Magnetic frustration and spontaneous rotational symmetry breaking in $PdCrO_2$, Phys. Rev. B **100**, 094414 (2019).

[16] E. V. Komleva, V. Y. Irkhin, I. V. Solovyev, M. I. Katsnelson, and S. V. Streltsov, Unconventional magnetism and electronic state in the frustrated layered system $PdCrO_2$, Phys. Rev. B **102**, 174438 (2020).

[17] V. Sunko, F. Mazzola, S. Kitamura, S. Khim, P. Kushwaha, O. J. Clark, M. D. Watson, I. Marković, D. Biswas, L. Pourovskii, T. K. Kim, T.-L. Lee, P. K. Thakur, H. Rosner, A. Georges, R. Moessner, T. Oka, A. P. Mackenzie, and P. D. C. King, Probing spin correlations using angle-resolved photoemission in a coupled metallic/Mott insulator system, Sci. Adv. **6**, eaaz0611 (2020).

[18] V. Sunko, P. H. McGuinness, C. S. Chang, E. Zhakina, S. Khim, C. E. Dreyer, M. Konczykowski, H. Borrmann, P. J. W. Moll, M. König, D. A. Muller, and A. P. Mackenzie, Controlled Introduction of Defects to Delafossite Metals by Electron Irradiation, Phys. Rev. X **10**, 021018 (2020).

[19] J. T. Chalker, Spin liquids and frustrated magnetism, in *Topological Aspects of Condensed Matter Physics*, edited by C. Chamon, M. Goerbig, R. Moessner, and L. Cugliandolo, Proceedings of the Les Houches Summer School of Theoretical Physics, CIII, 2014 (Oxford University Press, Oxford, UK, 2017), p. 123.

[20] C. M. Varma, P. B. Littlewood, S. Schmitt-Rink, E. Abrahams, and A. E. Ruckenstein, Phenomenology of the Normal State of Cu-O High-Temperature Superconductors, Phys. Rev. Lett. **63**, 1996 (1989).

[21] S. A. Hartnoll and A. P. Mackenzie, Colloquium: Planckian dissipation in metals, Rev. Mod. Phys. **94**, 041002 (2022).

[22] A. Keren, Dynamical Simulation of Spins on Kagomé and Square Lattices, Phys. Rev. Lett. **72**, 3254 (1994).

[23] R. Moessner and J. T. Chalker, Properties of a Classical Spin Liquid: The Heisenberg Pyrochlore Antiferromagnet, Phys. Rev. Lett. **80**, 2929 (1998).

[24] R. Moessner and J. T. Chalker, Low-temperature properties of classical geometrically frustrated antiferromagnets, Phys. Rev. B **58**, 12049 (1998).

[25] P. H. Conlon and J. T. Chalker, Spin Dynamics in Pyrochlore Heisenberg Antiferromagnets, Phys. Rev. Lett. **102**, 237206 (2009).

[26] A. M. Samarakoon, A. Banerjee, S. S. Zhang, Y. Kamiya, S. E. Nagler, D. A. Tennant, S. H. Lee, and C. D. Batista, Comprehensive study of the dynamics of a classical Kitaev spin liquid, Phys. Rev. B **96**, 134408 (2017).

[27] X. Bai, J. A. M. Paddison, E. Kapit, S. M. Koohpayeh, J. J. Wen, S. E. Dutton, A. T. Savici, A. I. Kolesnikov, G. E. Granroth, C. L. Broholm, J. T. Chalker, and M. Mourigal, Magnetic Excitations of the Classical Spin Liquid $MgCr_2O_4$, Phys. Rev. Lett. **122**, 097201 (2019).

[28] S. Zhang, H. J. Changlani, K. W. Plumb, O. Tchernyshyov, and R. Moessner, Dynamical Structure Factor of the Three-Dimensional Quantum Spin Liquid Candidate $NaCaNi_2F_7$, Phys. Rev. Lett. **122**, 167203 (2019).

[29] O. Franke, D. Călugăru, A. Nunnenkamp, and J. Knolle, Thermal spin dynamics of Kitaev magnets: Scattering continua and magnetic field induced phases within a stochastic semiclassical approach, Phys. Rev. B **106**, 174428 (2022).

[30] See Supplemental Material at http://link.aps.org/supplemental/10.1103/PhysRevB.107.L020402 for details on the numerical evaluation and fitting procedure for the spin structure factor, the fluctuation-dissipation theorem, the numerical evaluation of the electron self-energy with and without the local approximation, the filling dependence of the electron self-energy, and the procedure to determine the spin bandwidth for the simplified analytical approximation.

[31] Z. Wang, K. Barros, G.-W. Chern, D. L. Maslov, and C. D. Batista, Resistivity Minimum in Highly Frustrated Itinerant Magnets, Phys. Rev. Lett. **117**, 206601 (2016).

[32] D. Loison, C. Qin, K. Schotte, and X. Jin, Canonical local algorithms for spin systems: Heat bath and Hasting's methods, Eur. Phys. J. B **41**, 395 (2004).

[33] C. W. Hicks, A. S. Gibbs, L. Zhao, P. Kushwaha, H. Borrmann, A. P. Mackenzie, H. Takatsu, S. Yonezawa, Y. Maeno, and E. A. Yelland, Quantum oscillations and magnetic reconstruction in the delafossite $PdCrO_2$, Phys. Rev. B **92**, 014425 (2015).

[34] P. A. Lee, T. M. Rice, and P. W. Anderson, Fluctuation Effects at a Peierls Transition, Phys. Rev. Lett. **31**, 462 (1973).

[35] A. Georges, G. Kotliar, W. Krauth, and M. J. Rozenberg, Dynamical mean-field theory of strongly correlated fermion systems and the limit of infinite dimensions, Rev. Mod. Phys. **68**, 13 (1996).

[36] A. L. Chernyshev and O. A. Starykh, Roller Coaster in a Flatland: Magnetoresistivity in Eu-Intercalated Graphite, Phys. Rev. X **12**, 021010 (2022).